PHOTODYNAMIC THERAPY WITH METHYLENE BLUE AND CHLORIN e6 PHOTOSENSITIZERS: STUDY ON EHRLICH CARCINOMA MICE MODEL

Pominova D.V.[1,2], Ryabova A.V.[1,2], Skobeltsin A.S.[1], Markova I.V.[2], Romanishkin I.D.[1]
[1]Prokhorov General Physics Institute of Russian Academy of Sciences, Moscow, Russia
[2]National Research Nuclear University MEPhI (Moscow Engineering Physics Institute), Moscow, Russia

Abstract

Hypoxia negatively affects the effectiveness of all types of anticancer therapy, in particular photodynamic therapy (PDT). In this regard, various approaches to overcome the limitations associated with hypoxia are widely discussed in the literature, one of them is the use of photosensitizers (PS) operating through the first mechanism of the photodynamic reaction, such as methylene blue (MB). Previously, we have demonstrated that MB can have a positive effect on tumor oxygenation. In this work, we investigated the photodynamic activity of MB and a combination of MB with chlorin e6 on a tumor in vivo using a model of Ehrlich carcinoma. PDT was studied with the joint and separate administration of chlorin e6 and MB. The accumulation and localization of MB and its combination with chlorin e6 in vivo was assessed using video fluorescence and spectroscopic methods, and the effect of laser exposure on accumulation was analyzed. After the PDT with chlorin e6, MB and a combination of MB with chlorin e6, a good therapeutic effect and a decrease in the tumor growth rate were observed compared to the control, especially in groups with PDT with MB and with the simultaneous administration of chlorin e6 and MB. The level of tumor oxygenation on days 3 and 5 after PDT was higher for groups with irradiation, the highest oxygenation on the 5th day after PDT was observed in the group with PDT only with MB. Phasor diagrams of tumors after PDT show a deviation from the metabolic trajectory and a shift towards a longer lifetimes compared to the control tumor, which indicates the presence of lipid peroxidation products. Thus, tumor regression after PDT is associated with the direct destruction of tumor cells under the influence of reactive oxygen species formed during PDT. Thus, the effectiveness of PDT with the combined use of MB and chlorin e6 has been demonstrated, and the main mechanisms of the antitumor effect of the combination of these PS have been studied.

Keywords: photodynamic therapy, methylene blue, inhibition of tumor growth.

Contacts: Pominova D.V., e-mail: pominovadv@gmail.com

For citations: Pominova D.V., Ryabova A.V., Skobeltsin A.S., Markova I.V., Romanishkin I.D. Photodynamic therapy with methylene blue and chlorin e6 photosensitizers: study on Ehrlich carcinoma mice model, *Biomedical Photonics*, 2024, vol. 13, no. 2, pp. 9–18. doi: 10.24931/2413–9432–2024–13–2-9–18.

ФОТОДИНАМИЧЕСКАЯ ТЕРАПИЯ С ФОТОСЕНСИБИЛИЗАТОРАМИ МЕТИЛЕНОВЫЙ СИНИЙ И ХЛОРИН e6: ИССЛЕДОВАНИЕ НА МЫШИНОЙ МОДЕЛИ КАРЦИНОМЫ ЭРЛИХА

Д.В. Поминова[1,2], А.В. Рябова[1,2], А.С. Скобельцин[1], И.В. Маркова[2], И.Д. Романишкин[1]
[1]Институт общей физики им. А. М. Прохорова Российской академии наук, Москва, Россия
[2]Национальный исследовательский ядерный университет «МИФИ», Москва, Россия

Резюме

Гипоксия негативно влияет на эффективность всех видов противоопухолевой терапии, в частности фотодинамической терапии (ФДТ). В связи с этим в литературе широко обсуждаются разные подходы для преодоления ограничений, связанных с гипоксией. Одним из них является использование фотосенсибилизаторов (ФС), работающих по первому механизму фотодинамической реакции, таких как метиленовый синий (МС). Ранее нами было показано, что МС может положительно влиять на оксигенацию опухоли. В данной работе мы провели исследование фотодинамической активности МС и МС в комбинации с хлорином е6 на опухоли *in vivo* на модели карциномы Эрлиха. Была исследована ФДТ при совместном и раздельном введении хлорина е6 и МС. Выполнена оценка накопления и локализации МС и МС в комбинации с хлорином е6 *in vivo* при помощи видеофлуоресцентных и спектроскопических методов, проанализировано влияние лазерного воздействия на накопление. После проведения ФДТ с хлорином е6, МС и комбинации МС с хлорином е6 отмечен хороший терапевтический эффект и уменьшение скорости роста опухоли по сравнению с контролем, особенно

в группах с ФДТ с МС и при одновременном введении хлорина е6 и МС. Уровень оксигенации опухоли на 3-е и 5-е сутки после ФДТ был выше в группах с облучением, самая высока оксигенация на 5-е сутки после ФДТ отмечена в группе с ФДТ с МС. На фазорных диаграммах опухолей после проведения ФДТ наблюдается отклонение от метаболической траектории и сдвиг в сторону более длинного времени жизни по сравнению с контрольной опухолью, что указывает на наличие продуктов перекисного окисления липидов. Следовательно, регрессия опухоли после ФДТ связана с прямым разрушением опухолевых клеток под воздействием активных форм кислорода, образующихся при ФДТ. Таким образом, продемонстрирована эффективность ФДТ при совместном применении МВ и хлорина е6 и исследованы основные механизмы противоопухолевого действия комбинации этих ФС.

Ключевые слова: фотодинамическая терапия, метиленовый синий, подавление роста опухоли.

Контакты: Поминова Д.В., e-mail: pominovadv@gmail.com

Для цитирования: Поминова Д.В., Рябова А.В., Скобельцин А.С., Маркова И.В., Романишкин И.Д. Фотодинамическая терапия с фотосенсибилизаторами метиленовый синий и хлорин е6: исследование на мышиной модели карциномы Эрлиха // Biomedical Photonics. – 2024. – Т. 13, № 2. – С. 9–18.. doi: 10.24931/2413–9432–2024–13–2-9–18.

Introduction

Hypoxia is commonly associated with poor outcome in most cancer types and treatment modalities [1, 2, 3]. In recent years, it was shown that hypoxia plays an important role in the interaction between cancer cells, stroma and immune cells [4, 5, 6]. Hypoxia inducible factors (HIFs) are the major regulators of cancer cell survival [7, 8, 9, 10] and the role of hypoxia can be crucial in treatment resistance [11, 12].

Strategies to overcome hypoxia are widely discussed in many papers and reviews [13, 14, 15]. Strategies to increase oxygenation during photodynamic therapy (PDT), a promising approach for cancer treatment with low systemic toxicity and minimal invasiveness that has already demonstrated efficacy and safety in clinical use, are gaining increasing attention [16, 17, 18, 19]. During PDT, a special drug – photosensitizer (PS) – generates reactive oxygen species (ROS) under the action of light, which can damage biological structures and act as regulators of cell proliferation, metabolism, and apoptosis [20]. There are two types of reactions that result in the formation of ROS: the participation of PS in electron transfer reactions initiating the formation of hydroxyl radicals and hydroperoxides (type I photochemical reaction) and the energy transfer from PS to molecular oxygen, which results in the creation of singlet oxygen (type II photochemical reaction) [21]. The majority of clinically approved photosensitizers utilize the type II photochemical reaction, but less oxygen-dependent type I PDT is discussed as a strategy for the treatment of hypoxic tumors [22, 23]. Other strategies to overcome tumor hypoxia for enhancing PDT efficacy were summarized in recent review [24] and include delivering exogenous oxygen to tumor, generation of oxygen in tumor, reducing tumor oxygen consumption, normalizing tumor vasculature and inhibiting HIF-1 signaling pathway to relieve tumor hypoxia.

Our previous studies have shown that the methylene blue (MB) PS can be used to increase oxygenation of tumors via its redox properties [25, 26]. We assume that the changes in oxygenation are caused by interaction of MB with NADH [26, 27, 28]. A high ratio NADH/NAD^+ has been reported to be a key feature of malignant cells [29] and can reflect the inhibition of the electron transport chain [30]. When interacting with NADH, MB is reduced to the leucoform, while and NADH is oxidized to NAD^+, providing an increase of pyruvate:lactate (associated with shift from glycolysis to oxidative phosphorylation) and alpha-ketoglutarate (α-KG) to 2- hydroxyglutarate (HG) ratio (associated with decrease of reductive stress), suppression of 2-HG production [31] and reactivation of electron transport chain [30, 32]. The negative aspect is that he leucoform lacks absorption in the red part of the spectrum, making it photodynamically inactive. Consequently, the idea of utilizing a combination of two photosensitizers, MB and chlorin e6, to enhance the effectiveness of PDT arose. The intent is to increase the tumor oxygenation through the use of MB, and then carry out PDT with chlorin e6. In addition, the mutual influence of photosensitizers when administered together was studied, in particular, the effect of chlorin e6 on the transition of MB to the leucoform, as well as the synergistic effects caused by the use of two PS.

According to systematic review of preclinical studies [33] photodynamic therapy with MB is effective against different types of cancer including colorectal tumor, carcinoma, and melanoma. However, the results were promising not for all tumor types, a modest decrease in tumor size was observed for breast cancer and HeLa models, as well as no inhibition of osteosarcoma growth in mice [34]. Authors of review hypothesized that the bioavailability of MB in different target tissues is not equal. We assume that this may also be due to the transition of MB to the leucoform, which reduces its photodynamic activity.

Chlorin e6 is a second generation photosensitizer approved by FDA which has demonstrated high ROS generation ability and anticancer potency against many types of cancer [35]. It is commercially available and widely used for PDT in medical institutions in Russia [36, 37, 38].

Interest in the combined use of MB and chlorin e6 is due to the proximity of their absorption wavelengths in the near-infrared I part of the spectrum: 660 nm for chlorin e6 [39] and 664 nm for MB [40]. Excitation in this range allows for the reduction of autofluorescence and scattering from the biological tissue, thus facilitating deeper penetration into the tumor. The use of a single laser wavelength for both PS excitation is convenient and results in a production of a large number of ROS in the tumor cells and more effectively induces apoptosis, as was shown by Alimu et al [41]. However, this study was conducted on cells *in vitro* under normoxia conditions. In addition, liposomes loaded with two PS were studied, which, on the one hand, ensures simultaneous accumulation of drugs in the target area, but excludes the possibility of taking advantage of the effect of MB on tumor metabolism.

In this work, we conducted a study of PDT with the use of a combination of MB and chlorin e6 *in vivo* in a mouse model of Ehrlich carcinoma. *In vivo* research is of great importance because the oxygen distribution in tumors is highly heterogeneous, with hypoxia levels ranging from mild, almost non-hypoxic, to severe and anoxic levels [42]. The dynamic pattern of hypoxia levels that induces cellular responses and controls interactions between tumor cells, stroma and immune cells in the microenvironment cannot be simulated *in vitro* and at the same time is critical for assessing the effectiveness of photodynamic treatment. Intravenous joint and separate administration makes it possible to study the effect of each PS on the microenvironment and oxygenation, as well as the synergistic effects when two PS are used together.

Materials and methods

The photosensitizer used was a 0.35% solution of radachlorin (OOO RADAPHARMA, Russia) and a 1% aqueous solution of methylene blue (OJSC Samaramedprom, Russia).

Male BALB/c mice weighing 25–30 g and aged 8–10 weeks were used in experiments. The mice were kept in standard cages at a temperature of 21°C with a 12-hour light-dark cycle. They were given *ad libitum* access to standard laboratory feed and water. Ehrlich carcinoma was used as a model tumor; experiments were carried out on the 12th day after intramuscular grafting of the tumor onto the right hind paw. Tumor size was determined by direct measurement of its dimensions, and the volume was calculated using the formula: $V = 0.5 (L \times W^2)$, where V – volume, L – length and W – width. Tumor growth was assessed at the beginning of the experiment and on the third and fifth days after therapy. All measurements were done in triplicate. At the beginning of the experiment, the tumor size for all mice was about 1 cm^3.

The mice were divided into five groups based on concentrations of MB and chlorin e6 and irradiation dose. There were 4 groups with irradiation (wavelength 660 nm, light dose 60 J/cm^2): 1) with intravenous injection of 10 mg/kg of MB, 2) 5 mg/kg of e6, 3) 10 mg/kg of MB and 5 mg/kg of e6 simultaneously, 4) 5 mg/kg of e6 and 10 mg/kg of MB separately with the time interval between injection. The 200 µl of photosensitizer aqueous solution in saline with concentration calculated to achieve a total dose were administered intravenously into the tail vein under fluorescence control. Irradiation was carried out an hour after the introduction of photosensitizers. In the group with separate administration of MB and e6, chlorin e6 was first administered intravenously, an hour later MB and immediately irradiated. Groups with administration of 10 mg/kg MB, 5 mg/kg e6 without irradiation, as well as mice without administration of photosensitizers and irradiation were used as controls. Each group consisted of three mice.

The accumulation of MB, e6 and its combination in tumor was measured spectroscopically using a LESA-01-Biospec fiber-optic spectrometer (Biospec, Russia) with fiber-optic probe, consisting of a central illuminating fiber and six peripheral collecting fibers for the scattered and fluorescence radiation. MB fluorescence was excited with a He-Ne laser at 632.8 nm and 5 mW. Using an optical filter, the fluorescence was observed in the same dynamic range as the backscattered laser radiation. Fluorescence measurements were taken at five locations in tumor. After this, the data was averaged and STD was calculated. As a quantitative characteristic, we used the fluorescence index, calculated as the ratio of the area under the fluorescence peak in the range of 660-800 nm to the area under the laser peak in the range of 620-645 nm. The concentration of the PS in the tissues was calculated by matching the fluorescence index to the values from optical phantoms that mimic the scattering and absorption properties of biological tissues and contain a 0 to 10 mg/kg and 0 to 5 mg/kg range of MB and e6 concentrations, respectively.

For *in vivo* video imaging the PS fluorescence was excited using 660 nm laser radiation and detected by a black-and-white MQ013RG-ON camera (Ximea, Korea) with a 700–750 nm bandpass optical filter. The fluorescent signal was recorded in a video file, which was further processed. After the injection of the PS, the mouse remained under low-intensity laser irradiation for 5 minutes, during which the fluorescence signal was recorded to the video file. For the selected time-frames of the recorded video file, the average brightness in the tumor area was calculated. The brightness value in a pixel was normalized and took values from zero to one.

The degree of hemoglobin oxygenation *in vivo* was examined using a hemoglobin optical absorption method [43] with a halogen lamp as a light source. LESA-01-Biospec fiber-optic spectrometer was used to register the diffuse reflectance spectra. The degree of hemoglobin

oxygenation was calculated as the ratio of oxygenated hemoglobin absorption to total hemoglobin absorption, derived from the absorption spectrum. Oxygenation measurements were taken at five locations in both tumor and normal muscle tissue for each mouse.

The used spectroscopic methods and setup are described in more detail in the work [25].

To evaluate the effect of photodynamic therapy at the cellular level, the fluorescence microscopy and fluorescence lifetime imaging microscopy (FLIM) were used. Mice were euthanized on the fifth day after PDT. Tumors, subcutaneous tissue, skin, and muscle were excised en bloc and frozen. Sections of 50 μm were examined on a laser scanning confocal microscope LSM-710-NLO (Carl Zeiss AG, Oberkochen, Germany). The spectrally resolved images were acquired under simultaneous 488 nm and 633 nm laser excitation. Acridine orange (AO) and propidium iodide (PI) staining was used to assess the number of dead cells.

Time-resolved images of autofluorescence and MB fluorescence were recorded under two-photon 740 nm excitation with a Chameleon Ultra II femtosecond laser (Coherent, Saxonburg, Pennsylvania, USA), with a pulse width of 140 fs and a repetition rate of 80 MHz. Optical bandpass filters FB450-40 (Thorlabs, Newton New Hersey, USA) and BP 640/30 (Carl Zeiss AG, Oberkochen, Germany) were used to isolate fluorescence signals from NADH and MB, respectively. The images were processed with SPCImage 8.0 software (Becker & Hickl GmbH, Berlin, Germany). NADH metabolic index was calculated as a_1/a_2 ratio with fixed lifetimes: $\tau_1 = 0.4$ ns, $\tau_2 = 2.5$ ns [44].

Results and discussions

The therapeutic effects of MB and MB with chlorin e6 on tumors were investigated. *In vivo* fluorescence video imaging has shown that after intravenous administration, MB accumulates very quickly both in the tumor and in normal tissue, and then rapidly decreases in tumor, Fig. 1.

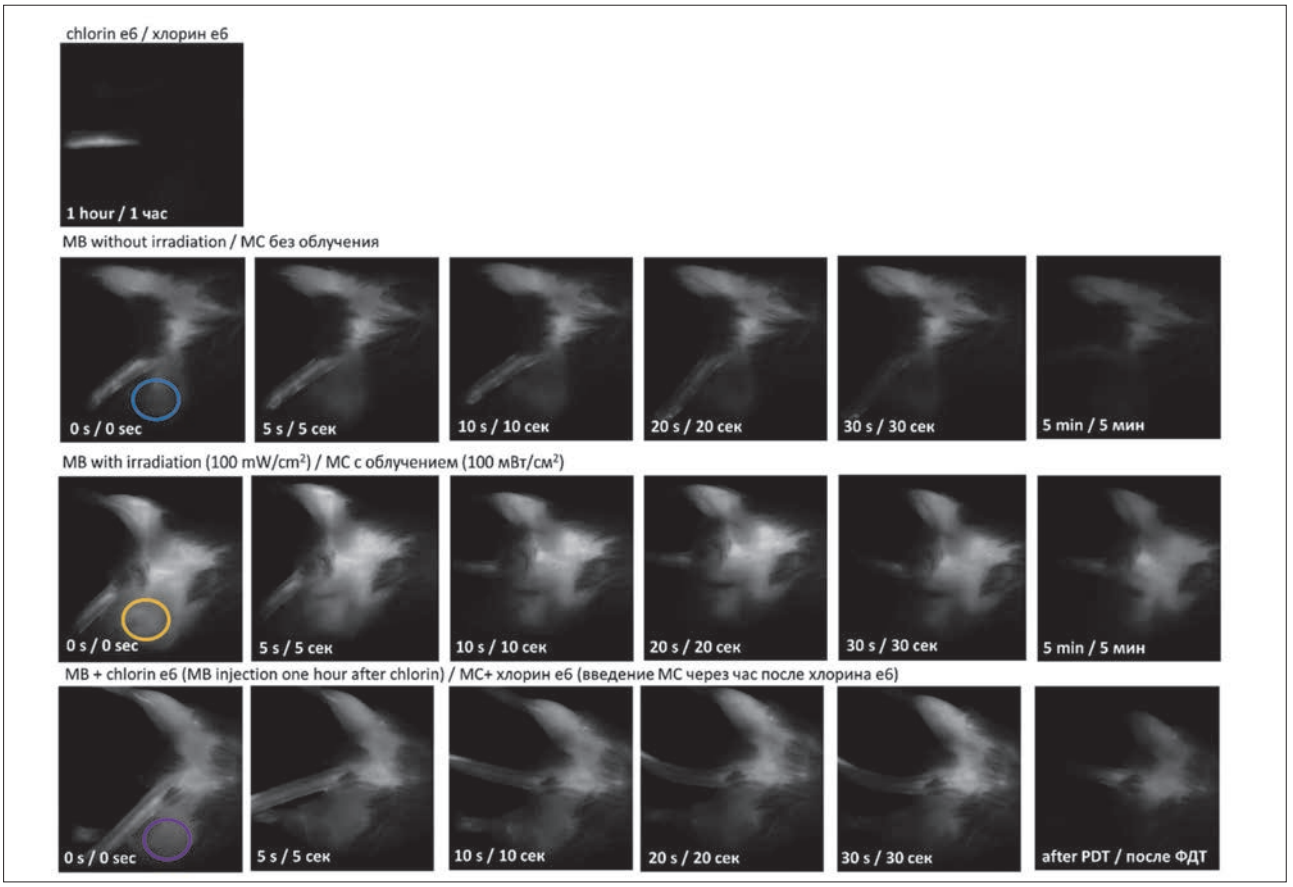

Рис. 1. Флуоресцентная визуализация МС in vivo с использованием возбуждения 660 нм: изображения, полученные через 5, 10, 20, 30 с и 5 мин после внутривенного введения МС в дозе 10 мг/кг и МС в комбинации с хлорином e6 (10 мг/кг + 5 мг/кг, введение МС произведено через 1 ч после введения хлорина e6). В группе с облучением каждые 5 с включали второй источник излучения с длиной волны 660 нм, плотность мощности 100 мВт/см^2. Цветные круги показывают области, в которых была рассчитана яркость.

Fig. 1. Fluorescence imaging of MB in vivo using 660 nm excitation: images obtained at 5, 10, 20, 30 seconds and 5 minutes after intravenous administration of MB at a dose of 10 mg/kg and MB in combination with chlorin e6 (10 mg/kg + 5 mg/kg, injection of MB was performed one hour after chlorin e6). In the irradiation group, a second radiation source with a wavelength of 660 nm and a power density of 100 mW/cm^2 was turned on every 5 seconds. The colored circles show the areas in which the brightness was calculated.

The fluorescence intensity of MB in normal tissues decreases slightly and remains constant throughout the entire measurement (5 minutes). These results are similar to the MB pharmacokinetics obtained in experiments on Lewis lung carcinoma [26].

The effect of laser irradiation and the second PS on the transition of MB to the leucoform was also analyzed. For quantitative assessment, the average brightness normalized to the initial value was used. The time dependences of the average brightness of tumor areas, normalized to the initial value, are presented in Fig. 2.

It can be seen that under the laser irradiation of MB, the decrease in fluorescence intensity occurs more slowly than for MB without irradiation. The same effect, but even more pronounced, was observed when MB is administered in combination with chlorin e6. We assume that irradiation prevents the transition of MB to the leucoform; during irradiation, the leucoform is reoxidized back to the MB upon interaction with reactive oxygen species.

Quantitative assessment of the accumulation of MB and chlorin e6 in the tumor was carried out using spectroscopic methods based on the fluorescence intensity in the red region of the spectrum recorded *in vivo*. The dependence of the fluorescence index on the accumulation time for tumors with intravenous administration is shown in Fig. 3.

The fluorescence intensity of chlorin e6 in the tumor gradually increases over time and reaches a plateau an hour after intravenous administration. The accumulation time of 1 hour for chlorin e6 was chosen for further experiments. The concentration of chlorin e6 in the tumor, determined by spectroscopic methods one hour after administration, was 0.7 mg/kg. An increase in the concentration of MB in the tumor was observed

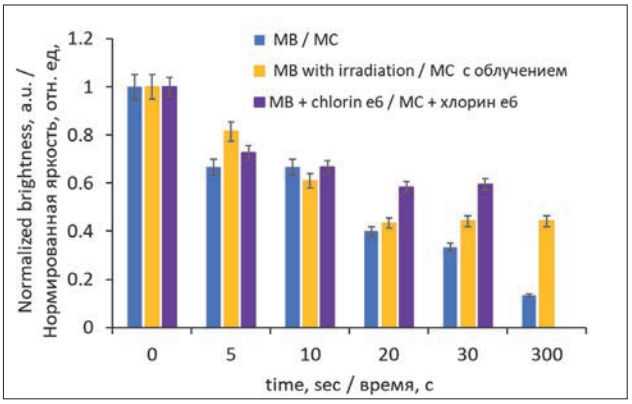

Рис. 2. Временные зависимости средней яркости опухоли, нормированной на начальное значение, для МС без облучения, МС с облучением (каждые 5 с включали второй источник излучения с длиной волны 660 нм, плотность мощности 100 мВт/см^2) и комбинации МС с хлорином e6.
Fig. 2. Time dependences of the average tumor brightness normalized to the initial value for MB without irradiation, MB with irradiation (every 5 seconds a second radiation source with a wavelength of 660 nm was turned on, power density 100 mW/cm^2) and a combination of MB with chlorin e6.

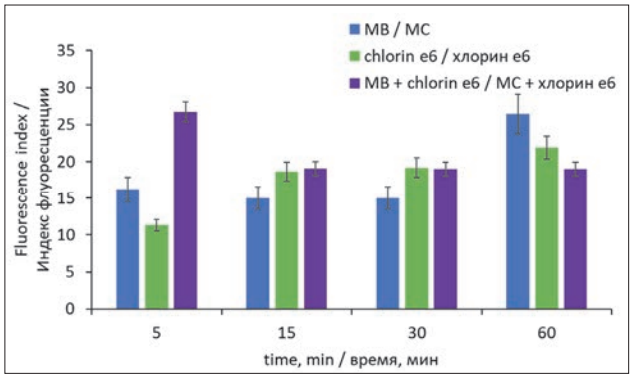

Рис. 3. Зависимость индекса флуоресценции МС, хлорина e6 и их комбинации в опухоли от времени накопления.
Fig. 3. Dependence of the fluorescence index for MB chlorin e6 and their combination in the tumor on the accumulation time.

only an hour after intravenous administration, which is presumably due to the transition to the leucoform 5 in minutes after administration, recorded using video fluorescent methods.

An interesting effect was observed for the combination of chlorin e6 and MB. Maximum of MB fluorescence was recorded immediately after the administration of PS, which corresponds to the data obtained using video fluorescent methods. The prevention of MB transition to the leucoform may also be due to the photodamaging effect of chlorin e6 on blood vessels, which occurred under low-intensity laser illumination during fluorescence imaging of PS accumulation. Another explanation for this effect could be a change in mitochondrial potential under the influence of chlorin e6, which leads to a disruption of MB reduction to the leucoform.

Changes in tumor oxygenation *in vivo* during PS accumulation were also assessed. For this study, a large tumor size was chosen; the volume before therapy was about 1 cm^3, oxygenation was significantly reduced relative to normal tissues and amounted to about 35%. The dependence of tumor oxygenation on PS accumulation time is shown in Fig. 4.

It has been shown that for Ehrlich carcinoma after intravenous administration of MB and a combination of MB with chlorin e6, a temporary decrease in oxygenation is observed, and then an increase in the level of oxygenation above the initial one. For the combination of chlorin e6 and MB, the increase in oxygenation levels occurred more quickly, as early as 30 minutes after administration, which correlates with faster accumulation of the PS combination. At the same time, the change in the level of oxygenation with the joint administration of MB and chlorin e6 was more pronounced, which confirms the assumption of the vascular effects of chlorin e6. Thus, it was previously shown that preliminary irradiation of a tumor with low-intensity laser radiation promotes more efficient accumulation of chlorin e6 [45].

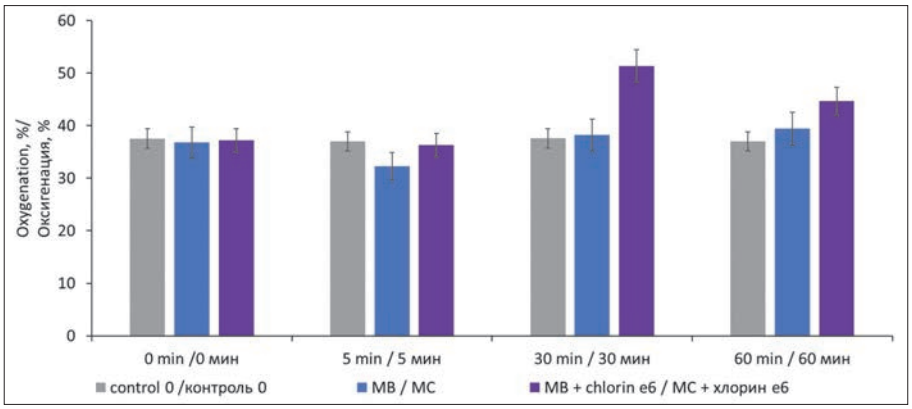

Рис. 4. Оксигенация опухоли, определенная по поглощению гемоглобина до, через 5, 30 мин и через 1 ч после внутривенного введения МС в дозе 10 мг/кг и комбинации МС с хлорином e6 (10 мг/кг + 5 мг/кг). Контроль – без введения ФС.
Fig. 4. Tumor oxygenation, determined by hemoglobin absorption before, after 5, 30 minutes and 1 hour after intravenous administration of MB at a dose of 10 mg/kg and a combination of MB with chlorin e6 (10 mg/kg + 5 mg/kg). Control – without administration of PS.

We have studied PDT with the combined use of chlorin e6 and MB. Based on the results obtained on the accumulation and effect on oxygenation, the following options for the joint use of drugs were chosen: joint administration of MB and chlorin e6 and laser irradiation an hour after administration (an increase in the tumor oxygenation and a more pronounced photodynamic effect was expected) and separate administration of PS, first chlorin e6 was injected, after an hour MB and immediately after MB administration was performed irradiation, until MB passes into a colorless form (an enhanced photodynamic effect was assumed due to a higher concentration of PS). In addition, the generation of singlet oxygen by chlorin e6 can lead to the oxidation of the colorless leucoform of MB back to blue, and chlorin e6 can have an effect on blood vessels.

The characteristic appearance of tumors in groups on days 3 and 5 after PDT is presented in Fig. 5.

The effectiveness of therapy was assessed by the rate of tumor growth. After therapy, the fastest growth of tumors was observed in the control group; on day 5 the tumor volume exceeded 3.5 cm^3, Fig. 6.

In the groups without irradiation, there was no significant decrease in tumor growth rate compared to the control group without any therapy. We hypothesize that the effect of MB on tumor oxygenation after a single administration is too short-lived for therapeutic effect.

A good therapeutic effect was observed in all groups with irradiation. After PDT with chlorin e6, MB and a combination of MB with chlorin e6 a decrease in the tumor growth rate were observed compared to the control. The most pronounced therapeutic effect was observed

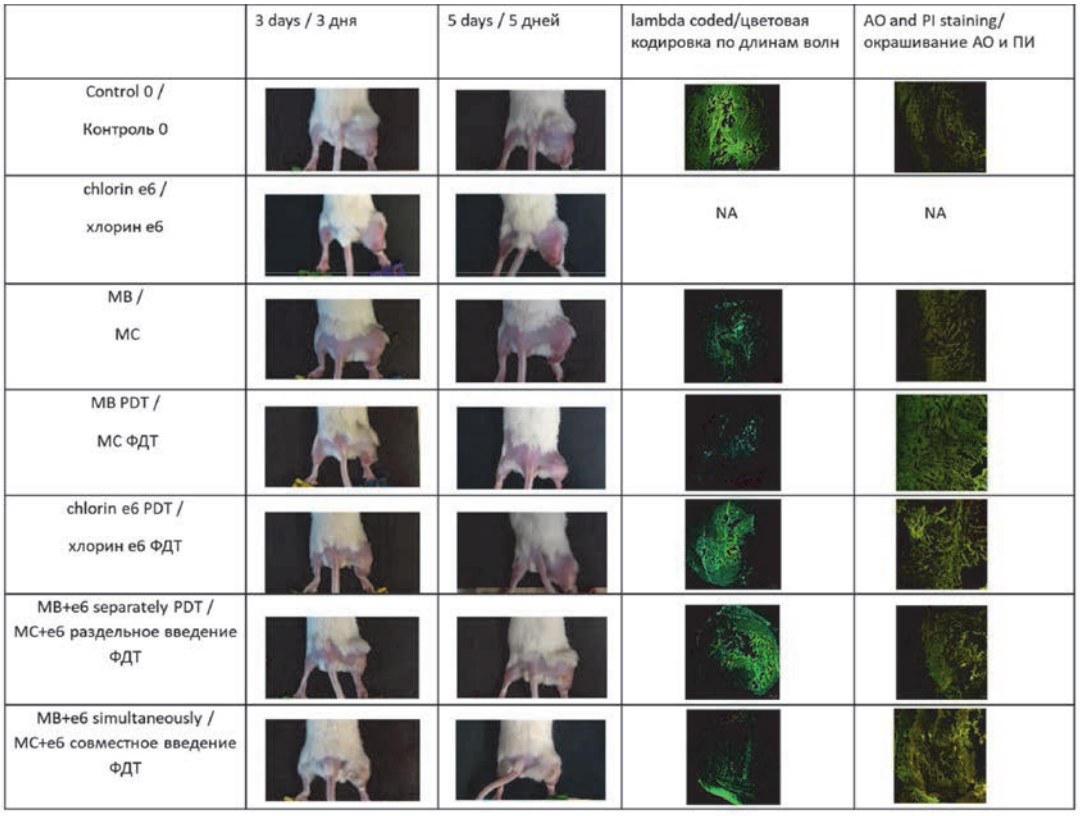

Рис. 5. Характерный вид опухоли в группах на 3-й и 5-й день после ФДТ. Флуоресцентные изображения криосрезов опухолей в режиме цветовой кодировки по длинам волн и после окрашивания акридиновым оранжевым и иодидом пропидия (АО и ПИ).
Fig. 5. Characteristic appearance in groups on the 3rd and 5th day after PDT. Fluorescent images of cryosections of tumors in wavelength-color-coded mode (lambda mode) and after staining with acridine orange and propidium iodide (AO and PI).

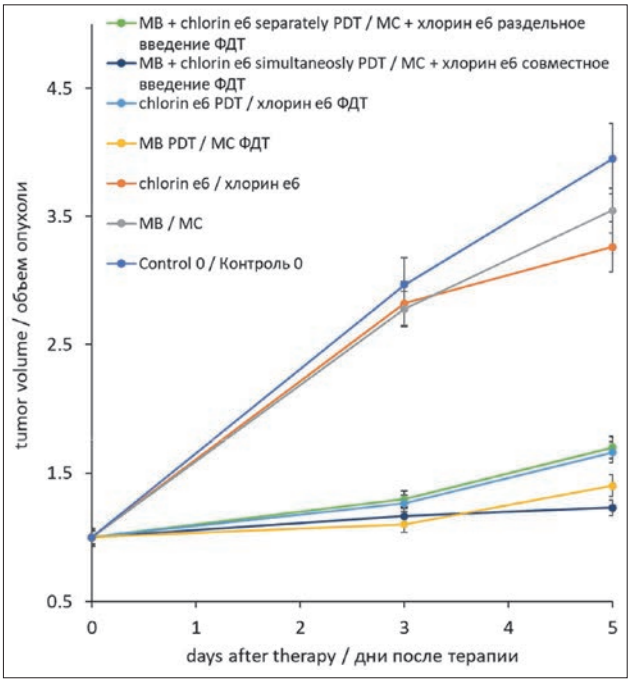

Рис. 6. Характерный размер опухоли в группах на 3-й и 5-й дни после ФДТ.
Fig. 6. Characteristic tumor size in groups on the 3rd and 5th day after PDT.

in groups with PDT with MB and with the simultaneous administration of chlorin e6 and MB (to increase tumor oxygenation before therapy) followed by irradiation an hour later. In both groups with the introduction of chlorin e6 and MB, the appearance of ulcers and more pronounced tissue necrosis in the area of photodynamic exposure were observed, however, the suppression of tumor growth was more significant in the group with the combined administration of MB and chlorin e6.

Oxygenation measurements were used as an additional parameter to assess the effectiveness of the therapy. The dependence of tumor oxygenation on time after PDT is shown in Fig. 7.

In all groups with irradiation, the level of tumor oxygenation on days 3 and 5 was higher than in the control group and groups without irradiation. The highest oxygenation on day 5 after PDT was observed for the group with MB and irradiation of 60 J/cm^2. The lower oxygenation for groups receiving chlorin e6 alone or in combination with MB is presumably due to the photodamaging effect of chlorin e6 on blood vessels.

Also, after animal euthanasia and preparation of cryosections of the studied tumors, FLIM was performed to study the effect of MB administration on the metabolic type of tumor tissues. The distribution of MB fluorescence

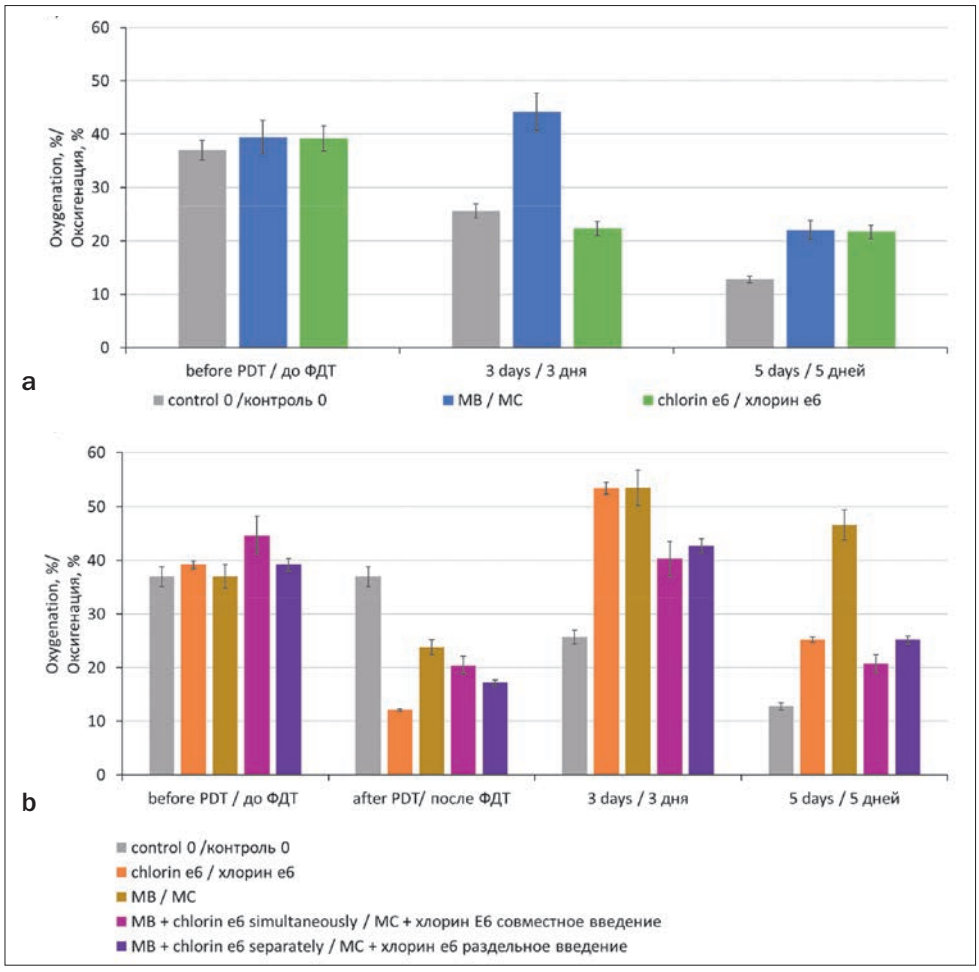

Рис. 7. Оксигенации опухоли, определенная по поглощению гемоглобина до ФДТ, сразу, на 3-й и 5-й дни после ФДТ для групп:
a – с облучением;
b – без облучения.
Fig. 7. The tumor oxygenation, determined by hemoglobin absorption before PDT, immediately, on days 3 and 5 after PDT for groups:
a – without irradiation;
b – with irradiation.

and the lifetime of the metabolic cofactor NADH were analyzed on cryosections of tumors.

Fig. 8 shows phasor diagrams of fluorescence in the spectral range of NADH from tumor sections.

Phasor diagrams of the FLIM for tumors after PDT show a deviation from the metabolic trajectory and a shift towards a longer lifetime compared to the control tumor without any therapy. This shift in the metabolic index indicates the presence of lipid peroxidation products [46]. Thus, tumor regression after PDT with studied PS is associated with the direct destruction of tumor cells under the influence of reactive oxygen species formed during PDT. Interestingly, more severe damage does not contribute to more effective suppression of tumor growth. Thus, in the group with PDT only with MB, for which the smallest shift in phasor was observed relative to the control, the suppression of tumor growth was most pronounced, along with the highest level of oxygenation on day 5 after therapy.

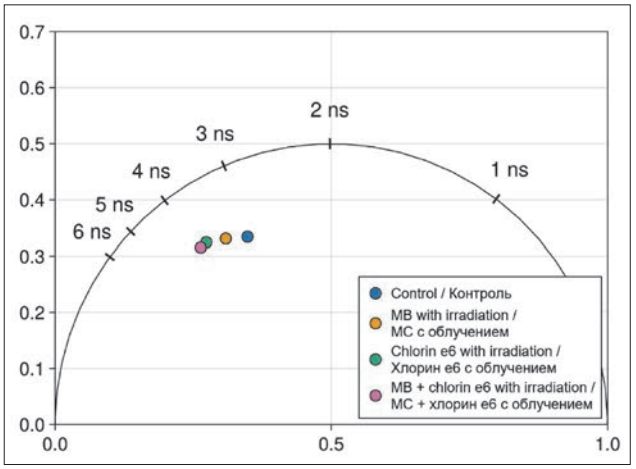

Рис. 8. Средние фазорные значения на разрешенных во времени флуоресцентных изображений НАДН в срезах опухоли после терапии.
Fig. 8. Mean phasor values for time-resolved fluorescence images of NADH in tumor cryosections after therapy.

Conclusion

A study was conducted of the therapeutic effects of MB and MB in combination with chlorin e6 on tumors *in vivo*.

Using spectroscopic methods, the optimal time for chlorin e6 accumulation in the tumor was estimated to be 1 hour. For MB, a smooth increase in concentration was observed with increasing accumulation time, which corresponds to the time dependence of MB concentration obtained previously for Lewis lung carcinoma. For the combination of chlorin e6 and MB, maximum accumulation was observed already 5 minutes after co-administration of the drugs, which is possibly due to the vascular effect of chlorin e6 during irradiation. Another explanation for this effect could be a change in mitochondrial potential under the influence of chlorin e6, which leads to a disruption in the reduction of MB to the leukemic form.

Study with help of video fluorescent methods confirmed previously obtained for Lewis carcinoma results: after intravenous administration, MB very quickly accumulates both in the tumor and in normal tissue. Irradiation of MB prevents the transition of MB to the leucoform, which is presumably due to the oxidation of LMB to MB upon interaction with reactive oxygen species. The same effect, but even more pronounced, is observed when MB is administered in combination with chlorin e6.

A study of the photodynamic activity of MB and MB in combination with chlorin e6 has demonstrated a good therapeutic effect and a decrease in the tumor growth rate for groups with PDT with chlorin e6, MB and a combination of MB with chlorin e6, a decrease in the tumor growth rate were observed in all groups with PDT compared to the control and groups without irradiation. The most pronounced therapeutic effect was observed in groups with MB and irradiation and with the combined administration of chlorin e6 and MB (to increase tumor oxygenation before therapy) followed by irradiation an hour later. In both groups with the introduction of chlorin e6 and MB, the appearance of ulcers and more pronounced tissue necrosis in the area of photodynamic exposure were observed, however, the suppression of tumor growth was more significant in the group with the combined administration of MB and chlorin e6.

The level of tumor oxygenation on days 3 and 5 was higher in groups with PDT compared to control and groups without irradiation. The highest oxygenation on day 5 after PDT was observed for the group with PDT with MB. The lower oxygenation for groups receiving chlorin e6 alone or in combination with MB is presumably due to the photodamaging effect of chlorin e6 on blood vessels.

Phasor diagrams of the FLIM for tumors after PDT show a deviation from the metabolic trajectory and a shift towards a longer lifetime compared to the control tumor. This shift in the metabolic index indicates the presence of lipid peroxidation products. Thus, tumor regression after PDT with studied PS is associated with the direct destruction of tumor cells under the influence of reactive oxygen species formed during PDT.

Thus, the effectiveness of PDT with combined use of MB and chlorin e6 was demonstrated. According to obtained results, the most promising approach among studied is the combined administration of chlorin e6 and MB to increase tumor oxygenation before therapy followed by irradiation an hour later. Further study is needed to optimize MB and chlorin e6 concentrations and accumulation time, as well as irradiation dose.

Acknowledgment

The study was funded by a grant from the Russian Science Foundation (project N 22-72-10117).

REFERENCES

1. Hockel M., Vaupel P. Tumor Hypoxia: Definitions and Current Clinical, Biologic, and Molecular Aspects, *JNCI Journal of the National Cancer Institute*, 2001, vol. 93 (4), pp. 266–276. doi:10.1093/jnci/93.4.266.
2. Vaupel P., Harrison L. Tumor Hypoxia: Causative Factors, Compensatory Mechanisms, and Cellular Response, *The Oncologist*, 2004, vol. 9 (S5), pp. 4–9. doi:10.1634/theoncologist.9-90005-4.
3. Robert Grimes D., Partridge M. A Mechanistic Investigation of the Oxygen Fixation Hypothesis and Oxygen Enhancement Ratio, *Biomed. Phys. Eng. Express*, 2015, vol. 1 (4), pp. 045209. doi:10.1088/2057-1976/1/4/045209.
4. Casazza A., Di Conza G., Wenes M. et al. Tumor Stroma: A Complexity Dictated by the Hypoxic Tumor Microenvironment, *Oncogene*, 2014, vol. 33 (14), pp. 1743–1754. doi:10.1038/onc.2013.121.
5. Bader S.B., Dewhirst M.W., Hammond E.M. Cyclic Hypoxia: An Update on Its Characteristics, Methods to Measure It and Biological Implications in Cancer, *Cancers*, 2020, vol. 13 (1), pp. 23. doi:10.3390/cancers13010023.
6. Vaupel P., Flood A.B., Swartz H.M. Oxygenation Status of Malignant Tumors vs. Normal Tissues: Critical Evaluation and Updated Data Source Based on Direct Measurements with pO2 Microsensors, *Appl Magn Reson*, 2021, vol. 52 (10), pp. 1451–1479. doi:10.1007/s00723-021-01383-6.
7. Zhang Q., Yan Q., Yang H. et al. Oxygen Sensing and Adaptability Won the 2019 Nobel Prize in Physiology or Medicine, *Genes & Diseases*, 2019, vol. 6 (4), pp. 328–332. doi:10.1016/j.gendis.2019.10.006.
8. Rankin E.B., Giaccia A.J. Hypoxic Control of Metastasis, *Science*, 2016, vol. 352 (6282), pp. 175–180. doi:10.1126/science.aaf4405.
9. LaGory E.L., Giaccia A.J. The Ever-Expanding Role of HIF in Tumour and Stromal Biology, *Nat Cell Biol*, 2016, vol. 18 (4), pp. 356–365. doi:10.1038/ncb3330.
10. Semenza G.L. Hypoxia-Inducible Factors in Physiology and Medicine, *Cell*, 2012, vol. 148 (3), pp. 399–408. doi:10.1016/j.cell.2012.01.021.
11. Jin M.-Z., Jin W.-L. The Updated Landscape of Tumor Microenvironment and Drug Repurposing, *Sig Transduct Target Ther*, 2020, vol. 5 (1), pp. 166. doi:10.1038/s41392-020-00280-x.
12. Krisnawan V.E., Stanley J.A., Schwarz J.K. et al. Tumor Microenvironment as a Regulator of Radiation Therapy: New Insights into Stromal-Mediated Radioresistance, *Cancers*, 2020, vol. 12 (10), pp. 2916. doi:10.3390/cancers12102916.
13. Sahu A., Kwon I., Tae G. Improving Cancer Therapy through the Nanomaterials-Assisted Alleviation of Hypoxia, *Biomaterials*, 2020, vol. 228, pp. 119578. doi:10.1016/j.biomaterials.2019.119578.
14. Ravichandran G., Yadav D.N., Murugappan S. et al. "Nano Effects": A Review on Nanoparticle-Induced Multifarious Systemic Effects on Cancer Theranostic Applications, *Mater. Adv.*, 2022, vol. 3 (22), pp. 8001–8011. doi:10.1039/D2MA00784C.
15. Zhao L., Fu C., Tan L. et al. Advanced Nanotechnology for Hypoxia-Associated Antitumor Therapy, *Nanoscale*, 2020, vol. 12 (5), pp. 2855–2874. doi:10.1039/C9NR09071A.
16. Mansoori B., Mohammadi A., Amin Doustvandi M. et al. Photodynamic Therapy for Cancer: Role of Natural Products, *Photodiagnosis and Photodynamic Therapy*, 2019, vol. 26, pp. 395–404. doi:10.1016/j.pdpdt.2019.04.033.
17. Correia J.H., Rodrigues J.A., Pimenta S. et al. Photodynamic Therapy Review: Principles, Photosensitizers, Applications, and Future Directions, *Pharmaceutics*, 2021, vol. 13 (9), pp. 1332. doi:10.3390/pharmaceutics13091332.
18. Jiang W., Liang M., Lei Q. et al. The Current Status of Photodynamic Therapy in Cancer Treatment, *Cancers*, 2023, vol. 15 (3), pp. 585. doi:10.3390/cancers15030585.
19. Olyushin V.E., Kukanov K.K., Nechaeva A.S. et al. Photodynamic Therapy in Neurooncology, *Biomedical photonics*, 2023, vol. 12 (3), pp. 25–35. doi:10.24931/2413-9432-2023-12-3-25-35.
20. Villalpando-Rodriguez G.E., Gibson S.B. Reactive Oxygen Species (ROS) Regulates Different Types of Cell Death by Acting as a Rheostat, *Oxidative Medicine and Cellular Longevity*, 2021, vol. 2021, pp. 1–17. doi:10.1155/2021/9912436.
21. Krasnovskiĭ A.A. [Photodynamic activity and singlet oxygen], *Biofizika*, 2004, vol. 49 (2), pp. 305–321.
22. Zhao X., Liu J., Fan J. et al. Recent Progress in Photosensitizers for Overcoming the Challenges of Photodynamic Therapy: From Molecular Design to Application, *Chem. Soc. Rev.*, 2021, vol. 50 (6), pp. 4185–4219. doi:10.1039/D0CS00173B.
23. Baptista M.S., Indig G.L. Effect of BSA Binding on Photophysical and Photochemical Properties of Triarylmethane Dyes, *J. Phys. Chem. B*, 1998, vol. 102 (23), pp. 4678–4688. doi:10.1021/jp981185n.

ЛИТЕРАТУРА

1. Hockel M., Vaupel P. Tumor Hypoxia: Definitions and Current Clinical, Biologic, and Molecular Aspects. // JNCI Journal of the National Cancer Institute. – 2001. – Т. 93, № 4. – С. 266–276.
2. Vaupel P., Harrison L. Tumor Hypoxia: Causative Factors, Compensatory Mechanisms, and Cellular Response. // The Oncologist. – 2004. – Т. 9, № S5. – С. 4–9.
3. Robert Grimes D., Partridge M. A mechanistic investigation of the oxygen fixation hypothesis and oxygen enhancement ratio. // Biomedical Physics & Engineering Express. – 2015. – Т. 1, № 4. – С. 045209.
4. Casazza A., Di Conza G., Wenes M., Finisguerra V., Deschoemaeker S., Mazzone M. Tumor stroma: a complexity dictated by the hypoxic tumor microenvironment. // Oncogene. – 2014. – Т. 33, № 14. – С. 1743–1754.
5. Bader S. B., Dewhirst M. W., Hammond E. M. Cyclic Hypoxia: An Update on Its Characteristics, Methods to Measure It and Biological Implications in Cancer. // Cancers. – 2020. – Т. 13, № 1. – С. 23.
6. Vaupel P., Flood A. B., Swartz H. M. Oxygenation Status of Malignant Tumors vs. Normal Tissues: Critical Evaluation and Updated Data Source Based on Direct Measurements with pO2 Microsensors. // Applied Magnetic Resonance. – 2021. – Т. 52, № 10. – С. 1451–1479.
7. Zhang Q., Yan Q., Yang H., Wei W. Oxygen sensing and adaptability won the 2019 Nobel Prize in Physiology or medicine. // Genes & Diseases. – 2019. – Т. 6, № 4. – С. 328–332.
8. Rankin E. B., Giaccia A. J. Hypoxic control of metastasis. // Science. – 2016. – Т. 352, № 6282. – С. 175–180.
9. LaGory E. L., Giaccia A. J. The ever-expanding role of HIF in tumour and stromal biology. // Nature Cell Biology. – 2016. – Т. 18, № 4. – С. 356–365.
10. Semenza G. L. Hypoxia-Inducible Factors in Physiology and Medicine. // Cell. – 2012. – Т. 148, № 3. – С. 399–408.
11. Jin M.-Z., Jin W.-L. The updated landscape of tumor microenvironment and drug repurposing. // Signal Transduction and Targeted Therapy. – 2020. – Т. 5, № 1. – С. 166.
12. Krisnawan V. E., Stanley J. A., Schwarz J. K., DeNardo D. G. Tumor Microenvironment as a Regulator of Radiation Therapy: New Insights into Stromal-Mediated Radioresistance. // Cancers. – 2020. – Т. 12, № 10. – С. 2916.
13. Sahu A., Kwon I., Tae G. Improving cancer therapy through the nanomaterials-assisted alleviation of hypoxia. // Biomaterials. – 2020. – Т. 228. – С. 119578.
14. Ravichandran G., Yadav D. N., Murugappan S., Sankaranarayanan S. A., Revi N., Rengan A. K. "Nano effects": a review on nanoparticle-induced multifarious systemic effects on cancer theranostic applications. // Materials Advances. – 2022. – Т. 3, № 22. – С. 8001–8011.
15. Zhao L., Fu C., Tan L., Li T., Zhong H., Meng X. Advanced nanotechnology for hypoxia-associated antitumor therapy. // Nanoscale. – 2020. – Т. 12, № 5. – С. 2855–2874.
16. Mansoori B., Mohammadi A., Amin Doustvandi M., Mohammadnejad F., Kamari F., Gjerstorff M. F., Baradaran B., Hamblin M. R. Photodynamic therapy for cancer: Role of natural products. // Photodiagnosis and Photodynamic Therapy. – 2019. – Т. 26. – С. 395–404.
17. Correia J. H., Rodrigues J. A., Pimenta S., Dong T., Yang Z. Photodynamic Therapy Review: Principles, Photosensitizers, Applications, and Future Directions. // Pharmaceutics. – 2021. – Т. 13, № 9. – С. 1332.
18. Jiang W., Liang M., Lei Q., Li G., Wu S. The Current Status of Photodynamic Therapy in Cancer Treatment. // Cancers. – 2023. – Т. 15, № 3. – С. 585.
19. Olyushin V. E., Kukanov K. K., Nechaeva A. S., Sklyar S. S., Vershinin A. E., Dikonenko M. V., Golikova A. S., Mansurov A. S., Safarov B. I., Rynda A. Y., Papayan G. V. Photodynamic therapy in neurooncology. // Biomedical Photonics. – 2023. – Т. 12, № 3. – С. 25–35.
20. Villalpando-Rodriguez G. E., Gibson S. B. Reactive Oxygen Species (ROS) Regulates Different Types of Cell Death by Acting as a Rheostat. // Oxidative Medicine and Cellular Longevity. – 2021. – Т. 2021. – С. 1–17.
21. Krasnovskiĭ A. A. [Photodynamic activity and singlet oxygen]. // Biofizika. – 2004. – Т. 49, № 2. – С. 305–321.
22. Zhao X., Liu J., Fan J., Chao H., Peng X. Recent progress in photosensitizers for overcoming the challenges of photodynamic therapy: from molecular design to application. // Chemical Society Reviews. – 2021. – Т. 50, № 6. – С. 4185–4219.
23. Baptista M. S., Indig G. L. Effect of BSA Binding on Photophysical and Photochemical Properties of Triarylmethane Dyes. // The Journal of Physical Chemistry B. – 1998. – Т. 102, № 23. – С. 4678–4688.
24. Wan Y., Fu L., Li C., Lin J., Huang P. Conquering the Hypoxia Limitation for Photodynamic Therapy. // Advanced Materials. – 2021. – Т. 33, № 48. – С. 2103978.

24. Wan Y., Fu L., Li C. et al. Conquering the Hypoxia Limitation for Photodynamic Therapy, *Advanced Materials*, 2021, vol. 33 (48), pp. 2103978. doi:10.1002/adma.202103978.
25. Pominova D.V., Ryabova A.V., Skobeltsin A.S. et al. Spectroscopic Study of Methylene Blue in Vivo: Effects on Tissue Oxygenation and Tumor Metabolism, *Biomedical photonics*, 2023, vol. 12 (1), pp. 4–13. doi:10.24931/2413-9432-2023-12-1-4-13.
26. Pominova D., Ryabova A., Skobeltsin A. et al. The Use of Methylene Blue to Control the Tumor Oxygenation Level, *Photodiagnosis and Photodynamic Therapy*, 2024, vol. 46, pp. 104047. doi:10.1016/j.pdpdt.2024.104047.
27. Sevcik P., Dunford H.B. Kinetics of the Oxidation of NADH by Methylene Blue in a Closed System, *J. Phys. Chem.*, 1991, vol. 95 (6), pp. 2411–2415. doi:10.1021/j100159a054.
28. Engbersen J.F.J., Koudijs A., Van Der Plas H.C. Reaction of NADH Models with Methylene Blue, *Recl. Trav. Chim. Pays-Bas*, 2010, vol. 104 (5), pp. 131–138. doi:10.1002/recl.19851040503.
29. Chiarugi A., Dölle C., Felici R. et al. The NAD Metabolome — a Key Determinant of Cancer Cell Biology, *Nat Rev Cancer*, 2012, vol. 12 (11), pp. 741–752. doi:10.1038/nrc3340.
30. Jiang H., Jedoui M., Ye J. The Warburg Effect Drives Dedifferentiation through Epigenetic Reprogramming, *Cancer Biol Med*, 2024, vol. 20 (12), pp. 891–897. doi:10.20892/j.issn.2095-3941.2023.0467.
31. Jiang H., Greathouse R.L., Tiche S.J. et al. Mitochondrial Uncoupling Induces Epigenome Remodeling and Promotes Differentiation in Neuroblastoma, *Cancer Research*, 2023, vol. 83 (2), pp. 181–194. doi:10.1158/0008-5472.CAN-22-1029.
32. Komlódi T., Tretter L. Methylene Blue Stimulates Substrate-Level Phosphorylation Catalysed by Succinyl–CoA Ligase in the Citric Acid Cycle, *Neuropharmacology*, 2017, vol. 123, pp. 287–298. doi:10.1016/j.neuropharm.2017.05.009.
33. Taldaev A., Terekhov R., Nikitin I. et al. Methylene Blue in Anticancer Photodynamic Therapy: Systematic Review of Preclinical Studies, *Front. Pharmacol.*, 2023, vol. 14, pp. 1264961. doi:10.3389/fphar.2023.1264961.
34. Matsubara T., Kusuzaki K., Matsumine A. et al. Methylene Blue in Place of Acridine Orange as a Photosensitizer in Photodynamic Therapy of Osteosarcoma, *In Vivo*, 2008, vol. 22 (3), pp. 297–303.
35. Hak A., Ali M.S., Sankaranarayanan S.A. et al. Chlorin E6: A Promising Photosensitizer in Photo-Based Cancer Nanomedicine, *ACS Appl. Bio Mater.*, 2023, vol. 6 (2), pp. 349–364. doi:10.1021/acsabm.2c00891.
36. Rynda A.Yu., Rostovtsev D.M., Olyushin V.E. et al. Therapeutic Pathomorphosis in Malignant Glioma Tissues after Photodynamic Therapy with Chlorin E6 (Reports of Two Clinical Cases), *Biomedical photonics*, 2020, vol. 9 (2), pp. 45–54. doi:10.24931/2413-9432-2020-9-2-45-54.
37. Filonenko E.V. Clinical Implementation and Scientific Development of Photodynamic Therapy in Russia in 2010-2020, *Biomedical photonics*, 2022, vol. 10 (4), pp. 4–22. doi:10.24931/2413-9432-2021-9-4-4-22.
38. Panaseykin Y.A., Kapinus V.N., Filonenko E.V. et al. Photodynamic Therapy Treatment of Oral Cavity Cancer in Patients with Comorbidities, *Biomedical photonics*, 2023, Vol. 11 (4), pp. 19–24. doi:10.24931/2413-9432-2022-11-4-19-24.
39. Adimoolam M.G., A. V., Nalam M.R. et al. Chlorin E6 Loaded Lactoferrin Nanoparticles for Enhanced Photodynamic Therapy, *J. Mater. Chem. B*, 2017, vol. 5 (46), pp. 9189–9196. doi:10.1039/C7TB02599H.
40. Lim D.-J. Methylene Blue-Based Nano and Microparticles: Fabrication and Applications in Photodynamic Therapy, *Polymers*, 2021, vol. 13 (22), pp. 3955. doi:10.3390/polym13223955.
41. Alimu G., Yan T., Zhu L. et al. Liposomes Loaded with Dual Clinical Photosensitizers for Enhanced Photodynamic Therapy of Cervical Cancer, *RSC Adv.*, 2023, Vol. 13 (6), pp. 3459–3467. doi:10.1039/D2RA03055A.
42. Hompland T., Fjeldbo C.S., Lyng H. Tumor Hypoxia as a Barrier in Cancer Therapy: Why Levels Matter, *Cancers*, 2021, vol. 13 (3), pp. 499. doi:10.3390/cancers13030499.
43. Stratonnikov A.A., Loschenov V.B. Evaluation of Blood Oxygen Saturation in Vivo from Diffuse Reflectance Spectra, *J. Biomed. Opt.*, 2001, vol. 6 (4), pp. 457. doi:10.1117/1.1411979.
44. Atamna H., Kumar R. Protective Role of Methylene Blue in Alzheimer's Disease via Mitochondria and Cytochrome c Oxidase, *JAD*, 2010, vol. 20 (s2), pp. S439–S452. doi:10.3233/JAD-2010-100414.
45. Efendiev K.T., Alekseeva P.M., Shiryaev A.A. et al. Preliminary Low-Dose Photodynamic Exposure to Skin Cancer with Chlorin E6 Photosensitizer, *Photodiagnosis and Photodynamic Therapy*, 2022, vol. 38, pp. 102894. doi:10.1016/j.pdpdt.2022.102894.
46. Datta R., Alfonso-García A., Cinco R. et al. Fluorescence Lifetime Imaging of Endogenou

25. Pominova D. V., Ryabova A. V., Skobeltsin A. S., Markova I. V., Romanishkin I. D., Loschenov V. B. Spectroscopic study of methylene blue in vivo: effects on tissue oxygenation and tumor metabolism. // Biomedical Photonics. – 2023. – Т. 12, № 1. – С. 4–13.
26. Pominova D., Ryabova A., Skobeltsin A., Markova I., Linkov K., Romanishkin I. The use of methylene blue to control the tumor oxygenation level. // Photodiagnosis and Photodynamic Therapy. – 2024. – Т. 46. – С. 104047.
27. Sevcik P., Dunford H. B. Kinetics of the oxidation of NADH by methylene blue in a closed system. // The Journal of Physical Chemistry. – 1991. – Т. 95, № 6. – С. 2411–2415.
28. Engbersen J. F. J., Koudijs A., Van Der Plas H. C. Reaction of NADH models with methylene blue. // Recueil des Travaux Chimiques des Pays-Bas. – 2010. – Т. 104, № 5. – С. 131–138.
29. Chiarugi A., Dölle C., Felici R., Ziegler M. The NAD metabolome — a key determinant of cancer cell biology. // Nature Reviews Cancer. – 2012. – Т. 12, № 11. – С. 741–752.
30. Jiang H., Jedoui M., Ye J. The Warburg effect drives dedifferentiation through epigenetic reprogramming. // Cancer Biology & Medicine. – 2024. – Т. 20, № 12. – С. 891–897.
31. Jiang H., Greathouse R. L., Tiche S. J., Zhao M., He B., Li Y., Li A. M., Forgo B., Yip M., Li A., Shih M., Banuelos S., Zhou M.-N., Gruber J. J., Rankin E. B., Hu Z., Shimada H., Chiu B., Ye J. Mitochondrial Uncoupling Induces Epigenome Remodeling and Promotes Differentiation in Neuroblastoma. // Cancer Research. – 2023. – Т. 83, № 2. – С. 181–194.
32. Komlódi T., Tretter L. Methylene blue stimulates substrate-level phosphorylation catalysed by succinyl–CoA ligase in the citric acid cycle. // Neuropharmacology. – 2017. – Т. 123. – С. 287–298.
33. Taldaev A., Terekhov R., Nikitin I., Melnik E., Kuzina V., Klochko M., Reshetov I., Shiryaev A., Loschenov V., Ramenskaya G. Methylene blue in anticancer photodynamic therapy: systematic review of preclinical studies. // Frontiers in Pharmacology. – 2023. – Т. 14. – С. 1264961.
34. Matsubara T., Kusuzaki K., Matsumine A., Satonaka H., Shintani K., Nakamura T., Uchida A. Methylene blue in place of acridine orange as a photosensitizer in photodynamic therapy of osteosarcoma. // In Vivo (Athens, Greece). – 2008. – Т. 22, № 3. – С. 297–303.
35. Hak A., Ali M. S., Sankaranarayanan S. A., Shinde V. R., Rengan A. K. Chlorin e6: A Promising Photosensitizer in Photo-Based Cancer Nanomedicine. // ACS Applied Bio Materials. – 2023. – Т. 6, № 2. – С. 349–364.
36. Rynda A. Yu., Rostovtsev D. M., Olyushin V. E., Zabrodskaya Yu. M. Therapeutic pathomorphosis in malignant glioma tissues after photodynamic therapy with chlorin e6 (reports of two clinical cases). // Biomedical Photonics. – 2020. – Т. 9, № 2. – С. 45–54.
37. Filonenko E. V. Clinical implementation and scientific development of photodynamic therapy in Russia in 2010-2020. // Biomedical Photonics. – 2022. – Т. 10, № 4. – С. 4–22.
38. Panaseykin Y. A., Kapinus V. N., Filonenko E. V., Polkin V. V., Sevrukov F. E., Isaev P. A., Ivanov S. A., Kaprin A. D. Photodynamic therapy treatment of oral cavity cancer in patients with comorbidities. // Biomedical Photonics. – 2023. – Т. 11, № 4. – С. 19–24.
39. Adimoolam M. G., A. V., Nalam M. R., Sunkara M. V. Chlorin e6 loaded lactoferrin nanoparticles for enhanced photodynamic therapy. // Journal of Materials Chemistry B. – 2017. – Т. 5, № 46. – С. 9189–9196.
40. Lim D.-J. Methylene Blue-Based Nano and Microparticles: Fabrication and Applications in Photodynamic Therapy. // Polymers. – 2021. – Т. 13, № 22. – С. 3955.
41. Alimu G., Yan T., Zhu L., Du Z., Ma R., Fan H., Chen S., Alifu N., Zhang X. Liposomes loaded with dual clinical photosensitizers for enhanced photodynamic therapy of cervical cancer. // RSC Advances. – 2023. – Т. 13, № 6. – С. 3459–3467.
42. Hompland T., Fjeldbo C. S., Lyng H. Tumor Hypoxia as a Barrier in Cancer Therapy: Why Levels Matter. // Cancers. – 2021. – Т. 13, № 3. – С. 499.
43. Stratonnikov A. A., Loschenov V. B. Evaluation of blood oxygen saturation in vivo from diffuse reflectance spectra. // Journal of Biomedical Optics. – 2001. – Т. 6, № 4. – С. 457.
44. Atamna H., Kumar R. Protective Role of Methylene Blue in Alzheimer's Disease via Mitochondria and Cytochrome c Oxidase. // Journal of Alzheimer's Disease. – 2010. – Т. 20, № s2. – С. S439–S452.
45. Efendiev K. T., Alekseeva P. M., Shiryaev A. A., Skobeltsin A. S., Solonina I. L., Fatyanova A. S., Reshetov I. V., Loschenov V. B. Preliminary low-dose photodynamic exposure to skin cancer with chlorin e6 photosensitizer. // Photodiagnosis and Photodynamic Therapy. – 2022. – Т. 38. – С. 102894.
46. Datta R., Alfonso-García A., Cinco R., Gratton E. Fluorescence lifetime imaging of endogenous biomarker of oxidative stress. // Scientific Reports. – 2015. – Т. 5, № 1. – С. 9848.